

Transfer Molding Technology for Smart Power Electronics Modules: Materials and Processes

K.-F. Becker,^{1,*} D. Joklitschke,¹ T. Braun,¹ M. Koch,¹ T. Thomas,² T. Schreier-Alt,¹ V. Bader,¹ J. Bauer,¹ T. Nowak,¹ O. Bochow-Ness,² R. Aschenbrenner,¹ M. Schneider-Ramelow,¹ and K.-D. Lang²

Abstract—In recent years, within power electronics packaging, there has been a trend toward compact power electronics modules for automotive and industrial applications, where a smart integrated control unit for motor drives is replacing bulky substrates with discrete control logic and power electronics. Most recent modules combine control and power electronics, yielding maximum miniaturization. Transfer molding is the method of choice for cost-effective encapsulation of such modules due to robustness of the molded modules and moderate cost of packaging. But there are challenges with this type of package.

Typically, these packages are asymmetric, and thus a substrate with single sided assembly is overmolded on the component side and the substrate backside is exposed, providing a heat path for optimized cooling. This asymmetric geometry is prone to yielding warped substrates, preventing optimum thermal contact to the heat sink and also putting thermomechanical stress on the encapsulated components, possibly reducing reliability.

Such packages are truly heterogeneous, combining power ICs, wire bonds, SMDs, control ICs, substrate, and lead frame surfaces. As a result, the encapsulant used needs to adhere sufficiently to all surfaces present.

Additionally, those packages need to operate at elevated temperatures for extended time periods, for example, at 150°C for 2000 h and more, so high thermal stability is of prime importance.

Within this paper, a reference application is described integrating power and control logic inside a lead frame based molded package. Taking into account the challenges mentioned above, a detailed description of material selection for this module will be given, including material analysis, such as rheology, reactivity, and change in ϵ_r ; and thermomechanical properties, in initial stage as $f(t, T)$ and after media storage. Process development tools for module molding are used to ensure manufacturability and usability. Concluding rules for encapsulant material selection and package setup are provided.

Keywords—Harsh environment, high temperature, smart power modules, transfer molding

INTRODUCTION

With evolving adaptation of System in Package (SiP) as a useful packaging approach, complexity is another driving characteristic for future developments in the field. Most of these systems are designed and built to embed intelligence and to enable the products in which they are used with the

ability to react to their environment and to provide relevant and ergonomic information to users. The amount of multimodal data to be processed by the system is very large. The user interfaces have to cope with complex and variable environments, while taking into account the context of use, and rapidly changing user behavior.

As far as technically and economically feasible, System on Chip solutions will be chosen, the adoption to various applications and the integration of highly complex systems containing nonelectronic functions will be carried out more cost-efficiently, with a high degree of miniaturization and flexibility in heterogeneous integration. Heterogeneous integration integrates several chips or components in one package (i.e., SiP) and carries out the interface to the application environment. Thus, heterogeneous integration is bringing nanoelectronics into broad application (Fig. 1) [1, 2].

Most electronic systems available today are realized through an organic printed wiring board, on which the individual components are placed. The wiring board is exclusively used with regard to electrical and mechanical function. However, necessity in the development of modern electronic products has led to the integration of further system functions into the board.

Future board and substrate technologies must ensure a cost-efficient integration of highly complex systems, with a high degree of miniaturization and sufficient flexibility in adaptation to different applications. Their functionality will be considerably enlarged by integration of non-electronic functions such as MEMS, antennas, or optical components. New production methods will ensure a high throughput at very low cost.

REFERENCE APPLICATION

Currently there is a strong focus on power electronics package development toward heterogeneous integration. This means the integration of a wide variety of components such as power ICs, shunts, microcontrollers, resistors, and capacitors on at least two types of substrates: ceramic or organic board and lead frame, ideally in a miniaturized conformation as described in the literature [3, 4]. As power electronics typically involves power loss and thus needs suitable thermal management, such packages need an exposed heat spreader that leads to an asymmetrical package geometry—a challenge when package warpage is an issue. Low warpage is necessary for good thermal interconnect between the heat spreader and the cooler. The package sizes are in the range of a $20 \times 20 \text{ mm}^2$ footprint.

Manuscript received June 2012 and accepted June 2012

¹Fraunhofer Institute for Reliability and Microintegration

²Technical University Berlin, Microperipheral Center, 13355 Berlin, Germany

*Corresponding author; email: karl-friedrich.becker@izm.fraunhofer.de

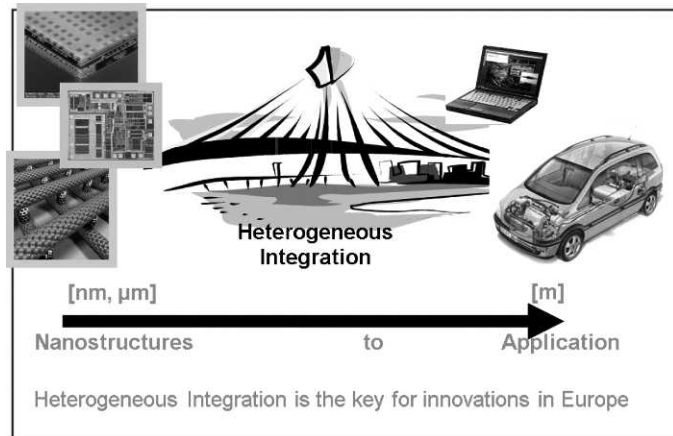


Fig. 1. Demand of future products for hetero system integration.

With differing heights, package volume can be estimated to be larger than 2000 mm^3 , that is, a big volume package with inhomogeneous internal structure can cause a long flow path for the encapsulant needed to protect the whole assembly.

As a reference application for smart power module research, a smart power module for maritime logistics has been defined at Fraunhofer IZM. Product functionality requires a smart driver module for an electromotor with $\sim 500 \text{ W}$ power. All control logic is to be integrated inside the module. The package is lead frame based with an integrated organic substrate carrying all the necessary discrete components and microcontrollers.

The project goal is to yield a miniaturized mold package using materials with high robustness and high temperature stability with optimized thermal performance. A sketch of the module is given in Fig. 2.

The challenges to be addressed with this package are the basic processability, that is, whether the module can be successfully encapsulated by transfer molding without air entrapments; the determination of thermal performance of the power module with a maximum junction temperature, T_j , of 140°C under the given boundary conditions; and last but not least, whether the module can withstand not only the standard demands of media resistance and thermal stability,

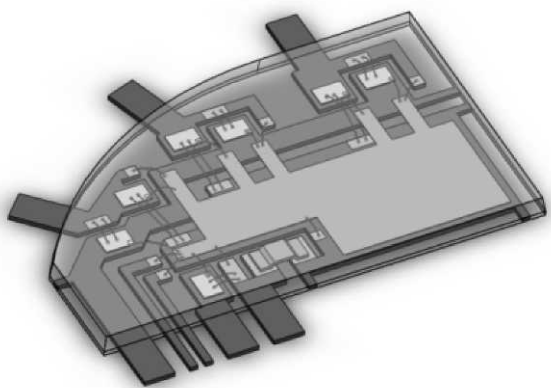


Fig. 2. Schematic drawing of a smart power module for maritime logistics/industrial application.

but also extreme conditions such as humidity, temperature, and media storage.

MATERIALS

For low-cost packaging of microelectronics, polymer materials are widely used, for example, as the substrate, adhesive, or encapsulant. Depending on the polymer class, these packages also have the potential for applications at elevated temperatures.

In summary, plastic encapsulation can be used for device encapsulation up to 200°C , but beyond that, there are only a limited number of material classes left, each with intrinsic advantages and disadvantages, so that high temperature use calls for careful selection.

Therefore, for this study, epoxy molding compounds (EMCs) were selected for detailed analysis and discussion as this class of material is suitable for highly reliable mass production with high application temperature potential.

EMCs are processed with transfer molding technology, an encapsulation process which is typically used for high volume production and which yields packages with high reliability, for example, the standard BGAs, QFPs, and TSOPs [5, 6]. This process and the materials are also used in automotive under-the-hood applications, and that is why this class of epoxy encapsulants was selected for the current investigation.

EMCs are supplied as one-component materials, where the epoxy resin and the hardener are already mixed. For optimized material properties, that is, those that have low coefficient of thermal expansion (CTE) and high glass transition temperature (T_g), typically SiO_2 filler particles in the range from 60-90 wt.% are added. Further additives are catalysts, adhesion promoters, colorants, surface wetting agents, or mold release substances.

For the investigations described here, a set of materials was chosen that is recommended by material suppliers exactly for the application of smart power modules with a maximum temperature of 150°C . Material properties are summarized in Table I. Those materials follow the general recommendations for smart power modules. First, a low CTE of $\sim 8 \text{ ppm/K}$ is necessary for minimum warpage of the modules, achieved by high degrees of filler content. This high filler content is achieved by using spherical particles with a wide size distribution down to the sub-micrometer scale, as depicted in Fig. 3. Second, a high adhesion to Cu and also to organics is needed to adapt to the heterogeneous internal structure of such packages.

Third, the materials are designed to fit into one of the T_g -concepts. Either low T_g materials are recommended with T_g values around 120°C to be compliant at elevated temperatures; or high T_g materials ($T_g > 180^\circ\text{C}$) are recommended to avoid a change in material properties within the temperature range of use.

METHODS

An important criterion for high package reliability is the thermomechanical mismatch of the packaging materials, which needs to be minimized. With this in mind, encapsulants are developed to have a low CTE or a high T_g . Since an electronic part in a car typically has to survive 10 years or more,

Table I
Material Parameters of EMCs Used for Evaluation—Materials A and B Are Recommended for Smart Power Modules, Data for Material C, a Standard Molding Compound Is Provided as a Reference (Datasheet Values)

Material	Material A	Material B	Material C, Reference
Filler content	90%	87%	72%
Filler type	Spherical, SiO ₂		50% spherical, 50% flakes
Maximum particle	75 μm		
Epoxy type	Biphenyl/MAR3		OCN
Hardener type	MAR		Phenol Novolac
Flame retardant	MAR		Sb
Spiral flow	90 cm	130-150 cm	80 cm
Gelation time	40 s	40 s at 175°C	40 s at 175°C
Flexural strength	0.18 GPa at RT, 0.022 GPa at 260°C		0.12 GPa at RT, 0.016 at 240°C
Flexural modulus	29 GPa at RT, 1 GPa at 260°C	15 GPa	125 GPa at RT, 1 GPa at 240°C
T_g	130°C	190°C	165°C
CTE α_1	8 ppm/°C	8 ppm/°C	17 ppm/°C
CTE α_2	32 ppm/°C	32 ppm/°C	6 ppm/°C
TC	1.0 W/m K		0.67 W/m K
Dielectric strength	20.1 kV/mm (2 mm)		
Water absorption	0.12%	0.39 wt.% (PCT 20 h)	0.38%
Specific gravity	2.03	2	1.81
Cure time	120 s	90 s	120 s
Mold temperature	175°C	175°C	175°C
Mold pressure	7-10 MPa	8 MPa	8.5 MPa
Post cure condition	4 h at 175°C	5 h at 175°C	4 h at 175°C
Mold shrinkage	0.12%	0.00%	

the material properties should roughly stay the same over this lifetime. But high temperatures, humidity, or aggressive fluids may cause an aging of the polymer.

- Chemical aging can lead to changes in molecular weight or cross link density of the 3D duromer network.
- Physical aging can decrease the specific volume and molecular free volume with a corresponding decrease in molecular mobility.

But the common effects of this aging are changes in mechanical properties such as increasing modulus and decreasing toughness. And this is directly linked to the package reliability.

Thermogravimetry (TGA) is the common method to characterize thermal and thermo-oxidative stability of materials, especially of polymers. Investigations were done with Q5000 IR TGA (TA Instruments) under air using a heating rate of 10 K/min from 30°C to 950°C. Furthermore, a long-term stability test was done starting with slow heating at 2 K/min to 280°C, followed by an isothermal step at 280°C for 18 h.

Dielectric spectroscopy (DEA) gives information on mobility and relaxation of dipoles and charges in dependence on frequency and temperature that can be correlated to structural changes of the sample [7]. Measurements of plate capacitors were done with a Novocontrol ALPHA-AN high resolution dielectric analyzer at a frequency of 1 kHz. The complex impedance

$$Z^* = \frac{U^*}{I^*}$$

with a real (Zp') and an imaginary (Zp'') part, the complex capacity

$$C^* = -\frac{i}{\omega Z^*}$$

with ($\omega = 2\pi f$), and the complex dielectric permittivity

$$\varepsilon^* = \frac{C^*}{C_0}$$

of the material, where C_0 is the capacity of the unfilled capacitor, were calculated from the measured data.

Dynamic mechanical analysis (DMA) was performed with a rheometer AR-G2 (TA Instruments) in oscillation mode at 1 Hz under a controlled strain of 0.1% on molded rectangular bars. The complex torsional modulus $G^* = G' + iG''$ and loss factor

$$\tan \delta = \frac{G''}{G'}$$

were calculated from measured data and sample geometry. The maximum of $\tan \delta$ in a temperature scan was used to define the T_g of the sample.

EXPERIMENT—MATERIAL DEGRADATION

The aim of the investigation was the determination of material stability under extreme conditions. The conditions were derived from previous investigations [8], where storage in test fuel, brake fluid (DOT 4), moisture, and high temperature storage were identified to have the strongest effect on the mechanical integrity of materials. Since test fuel is not present for the application targeted, it is also not used in this study. The test program performed includes a material analysis in the initial state and after media/temperature storage, while the storage conditions are as follows.

- Temperature storage at 225°C/250°C for 500 h and 1000 h under standard atmosphere.
- Storage in DOT 4 at 120°C for 500 h and 1000 h.

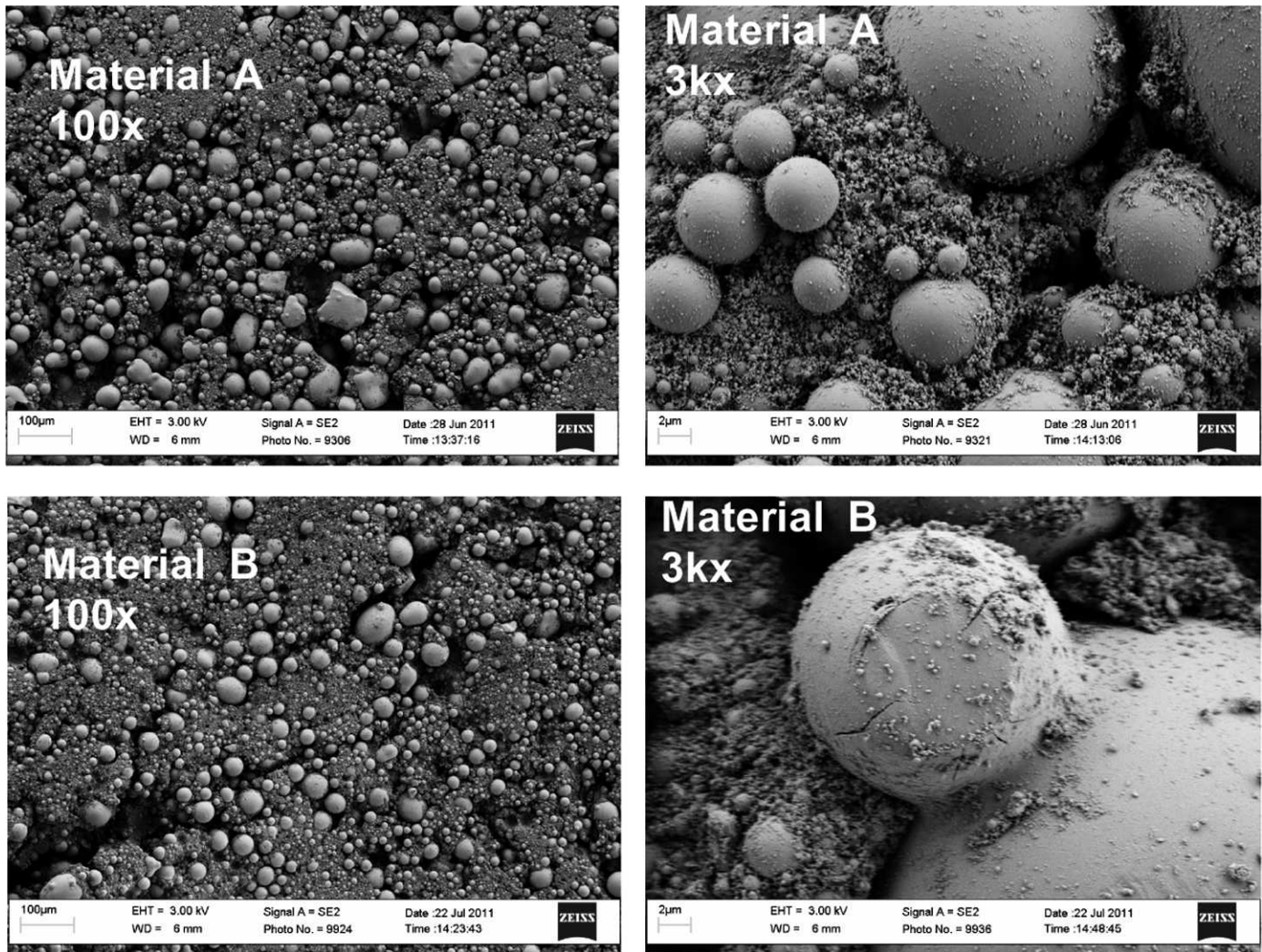


Fig. 3. SEM images of filler particles used for materials A and B. For both materials, the filler size distribution was found to be rather wide.

- Humidity storage at 85°C/85% relative humidity for 100 h, 250 h, 500 h, and 1000 h.
- Humidity storage inside a pressure cooker at 125°C and 100% relative humidity for 24 h.

The test methods used have been described in detail and are summarized briefly as follows.

- Determination of weight loss and degradation temperature using TGA.
- Determination of Young's modulus and T_g using a torsion test (sample geometry: $6 \times 0.5 \text{ mm}^2$ with a length of $\sim 40 \text{ mm}$).
- Determination of ϵ_r using DEA (sample geometry: $20 \times 20 \times 0.5 \text{ mm}^3$).

The first evaluation step consisted of the determination of degradation temperature of the materials to evaluate their potential to withstand high T storage. For both materials, the degradation temperature is around 400°C (see Fig. 4).

The TGA investigations under oxidizing and inert atmosphere showed that 1.5 wt.% higher loss occurs for material A under an oxidizing atmosphere, which can be explained by

the formation of nonvolatile residues under N_2 . On the other hand, material B degrades slightly slower at temperatures above 500°C under inert atmosphere, but nearly the same weight remains at 950°C.

The variation of weight loss between samples of material A with and without post cure (5 h at 175°C) indicates an evaporation of volatile content during this phase of 2 wt.%, a rather high value considering that there is only 10 wt.% of polymer material in the EMC. The weight loss curve of the post cured samples of material A stored in DOT 4 indicates that the matrix takes up about 3.4 wt.% of DOT 4, that is, desorbing below 400°C, where thermal degradation starts, comparable to the other samples (Fig. 5).

Taking a closer look at the thermomechanical properties of material A depicted in Figure 6, it can be seen that in the initial state, the material shows two peaks in $\tan \delta$, which is an indication for two network structures inside the polymer, each with a different T_g . After temperature and media storage, it can be seen that only slight changes occur after humidity storage, whereas high temperature as well as DOT 4 storage cause significant changes. High temperature storage results in

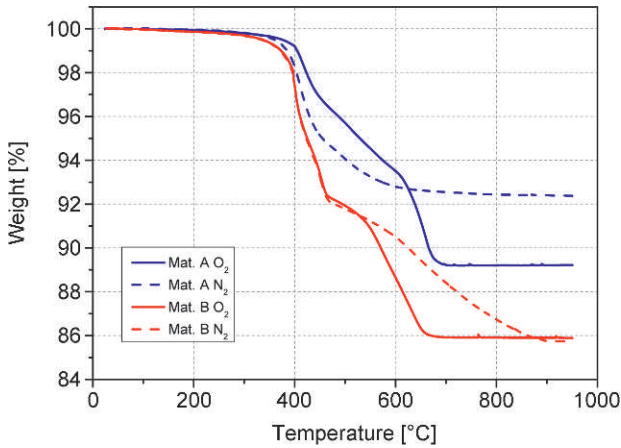


Fig. 4. TGA analysis of materials A and B in the initial state.

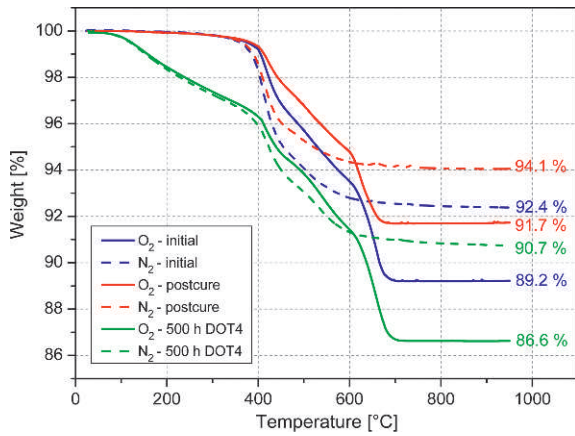


Fig. 5. TGA analysis of material A in the initial state and after media storage.

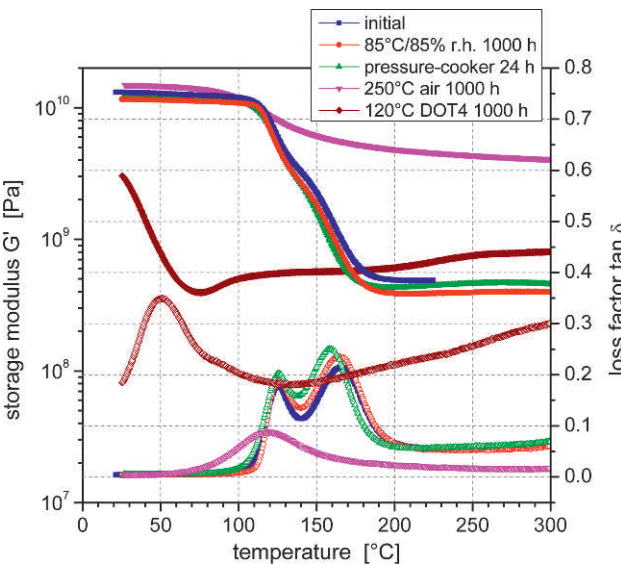


Fig. 6. Storage modulus G' and loss factor $\tan \delta$ of material A for various storage conditions.

only minor changes in the temperature range below T_g , but the storage modulus increases and the loss factor decreases in a wide temperature range above T_g , indicating embrittlement due to partial degradation and recombination of polymer chains.

On the other hand, a significant decrease of modulus and T_g as well as an increase of loss factor is observed for DOT 4 stored samples. This effect is most likely caused by the uptake of 4 wt.% DOT 4 into the matrix and the resulting softening effect, comparable to a flexibilizer used in thermoplastics.

Material B shows a partially different thermomechanical behavior (see Fig. 7).

The material has only one glass transition range at higher temperatures, compared with the double peak of the loss factor of material A, indicating a more uniform molecular structure. Storage under humidity leads to only minor changes and significant stiffening is the result of long term storage at 250°C.

In contrast to this nearly similar behavior of both materials, the effect of DOT 4 storage on the properties is significantly less for material B: only a slight decrease of T_g and storage

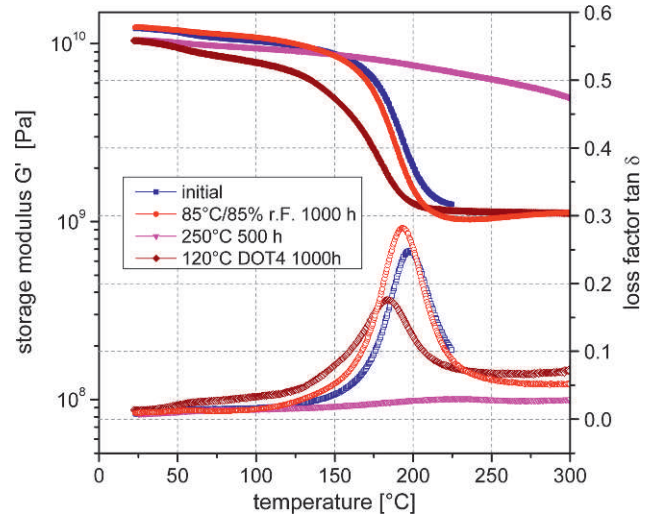


Fig. 7. Storage modulus G' and loss factor $\tan \delta$ of material B for various storage conditions.

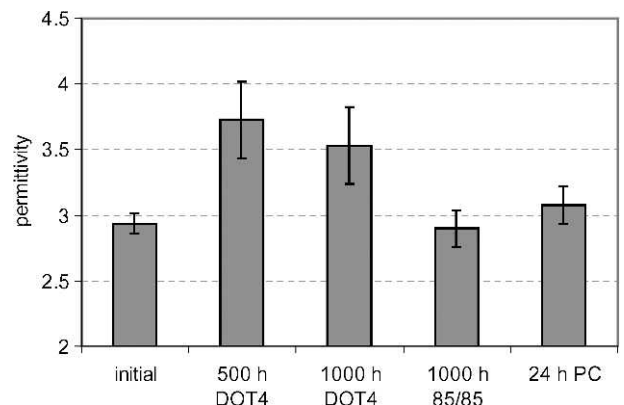


Fig. 8. Dielectric permittivity of material A after humidity and DOT 4 storage.

modulus could be detected compared with the major changes of material A.

Furthermore, the dielectric permittivity of samples in the initial state and after media storage was measured for material A (see Fig. 8). Only a minor influence was detected for humidity storage, whereas DOT 4 storage caused a significant increase of the dielectric constant, confirming the findings of TGA and DMA analysis.

Fig. 9 shows the results of a SEM analysis of samples of material A after different storage conditions.

These images also confirm the findings of the previous investigations. A cohesive fracture was found in the initial

state. Looking at the filler particles, they are typically covered by the matrix layer (Fig. 9, top). After temperature storage, the material becomes brittle and shrinks, resulting in delaminations between the matrix and the filler as shown in the middle of Fig. 9. The filler-matrix adhesion is also reduced by DOT 4 storage, probably caused by interface hydrolysis. This effect, shown in the bottom of Fig. 9, is similar to that found after thermal storage, but much stronger.

In summary, the compounds tested have distinct limits for their use under extreme conditions, but are estimated to withstand short-term exposure (<250 h) to temperature and humidity. Only storage in brake fluid, even for short times, at elevated temperature, is considered critical.

THERMAL SIMULATION

In order to evaluate the material selection with respect to thermal performance of the device, a thermal finite element model was generated to describe steady state heat conduction. All important materials are considered with their respective thermal conductivity. The device is mounted to a heat sink on one side and faces air on the other side with a constant temperature of 120°C. The bottom temperature is assumed to be constant at 110°C. In the load case, defined at the FETs (field effect transistors) and shunt with a sum heat loss of 14 W, the question is whether a high thermal conductivity EMC is needed, for which the criterion is a maximum junction temperature of 140°C. A model was generated to allow thermal simulation and is depicted in Fig. 10.

Molding compound was simulated to have standard thermal conductivity of 0.5 W/mK. The simulation result is depicted in Fig. 11. It was found that for the load case, the junction temperature of all components is well below 140°C, in fact, the junction temperature is even below 120°C. The dominant thermal path is through the die backside into the lead frame and then into the heat spreader, so the rather low thermal conductivity of EMC covering one side of the asymmetric package does not contribute too much to the resulting junction temperature. Therefore, the use of a compound with increased thermal conductivity (~2 W/mK) would not lead to significant improvement.

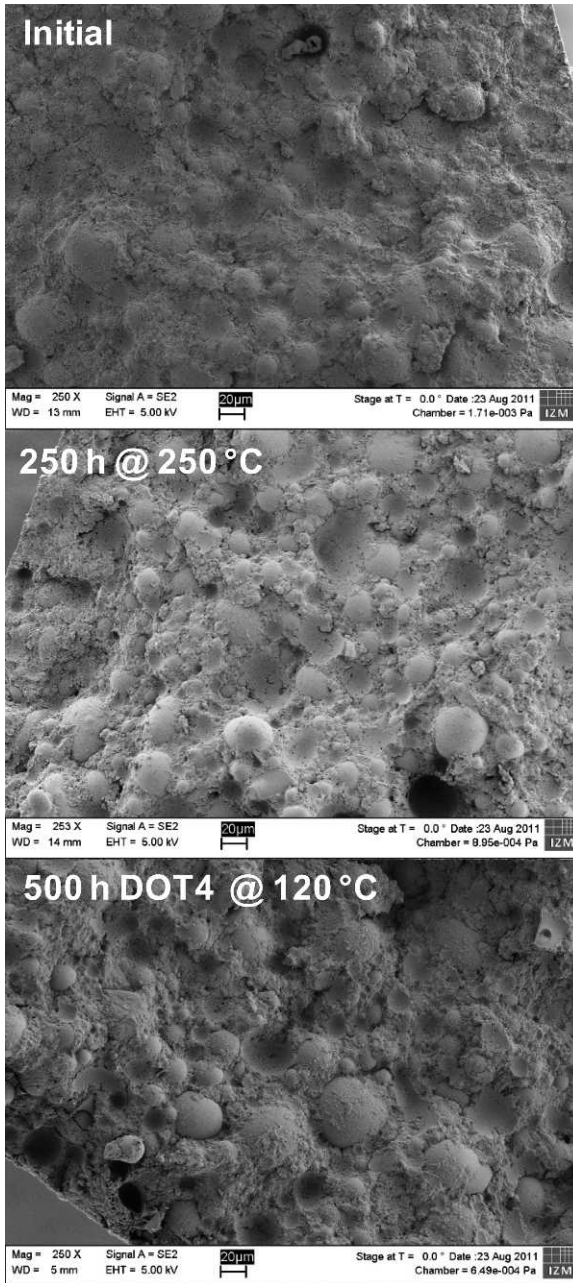


Fig. 9. SEM analysis of material A sample surface of fracture after various stages of aging. Top: initial. Middle: after 250 h at 250°C. Bottom: after 500 h DOT 4 storage at 120°C.

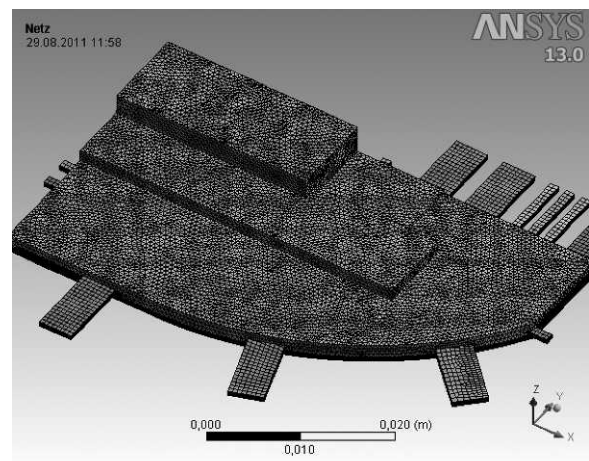


Fig. 10. Model used for thermal simulation.



Fig. 11. Thermal simulation results for low stress use case, where the junction temperature, T_j , is below 120°C.

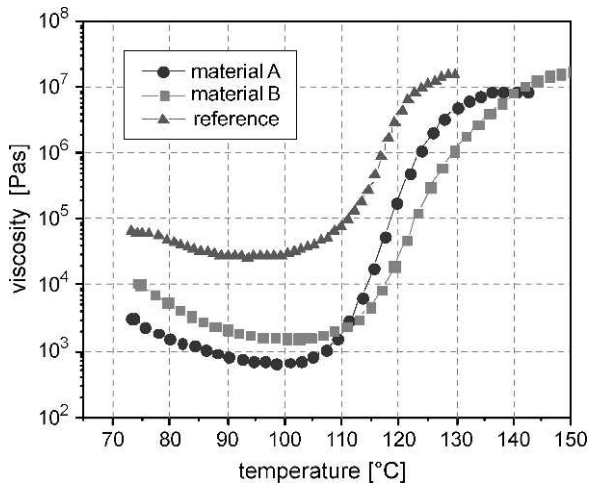


Fig. 12. Viscosity of materials A and B compared with reference material C during dynamic heating at 2 K/min.

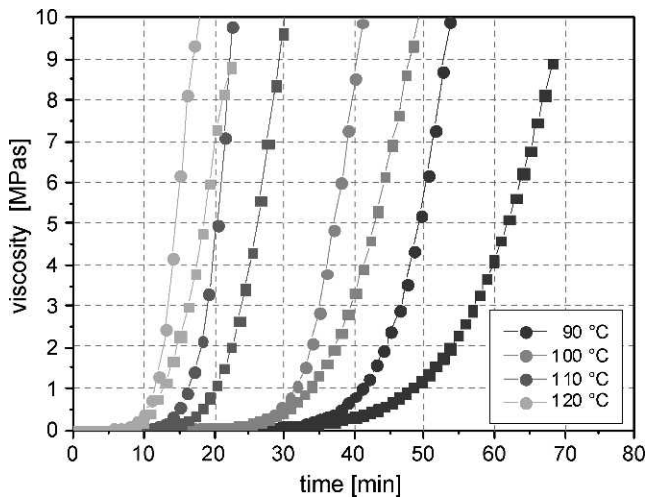


Fig. 13. Viscosity of material A (circles) and material B (squares) during isothermal cure at different temperatures.

FLOW SIMULATION

Numerical simulation of the polymer flow within narrow gaps has been, up to now, a challenging task for process engineers. First, the large number of small gaps between electronic parts, mold wall, and PCB have to be meshed precisely, heavily increasing the FEM computation time. Second, the filler particles within the polymer (up to 90 wt.%) can increase the flow resistance of the epoxy within small gaps and cause a separation between the filler and the polymer matrix. Nonuniform filler distribution can be a cause of failures such as cracks [9].

Commercially available tools for simulation of transfer molding are—as far as we know—not able to predict the filling behavior of polymers within thin (<500 μm), but wide-stretching gaps (>40 mm) precisely. Chen et al. [10] have observed viscosities of unfilled polymers within 200 μm wide gaps differing up to 75% from standard FEM predictions.

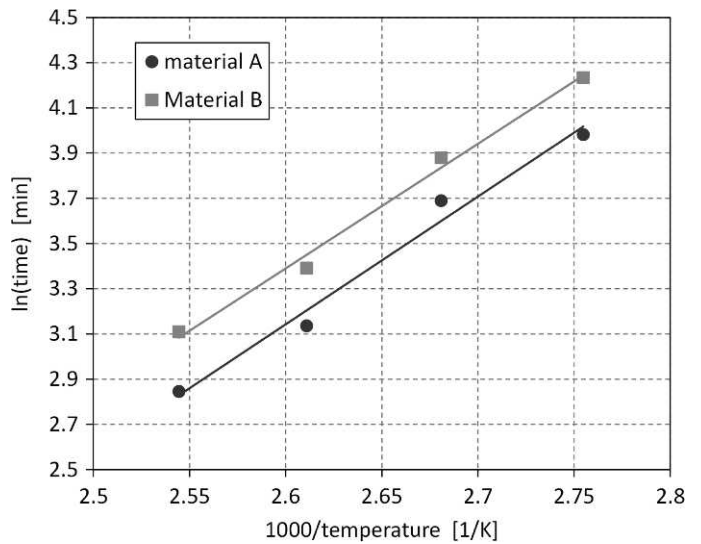


Fig. 14. Arrhenius plot of gel times of materials A and B from viscosity measurements.

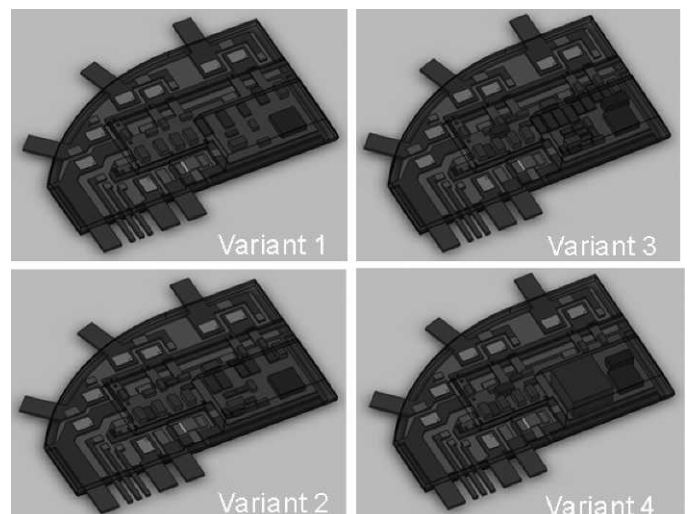


Fig. 15. Experimental setup for flow study using four component configurations.

Simulations show a more or less symmetrical flow pattern around the gate that does not change significantly if one of the following parameters changes: filler degree, viscosity η , injection pressure p , temperature of the melted epoxy T , or cavity height h .

Therefore, to allow a relevant simulation of flow behavior into a large volume package as it is investigated in this paper, first, a detailed analysis of flow and reaction properties of the encapsulants is necessary.

As an example, rheological measurements with materials A and B and reference material C with coarse filler particles are depicted in Fig. 12. Material A shows the lowest viscosity, but compared with the reference, both materials have relatively low viscosity due to their spherical filler particles that allow homogeneous and smooth flow.

The gelling behavior of materials A and B is compared in terms of their viscosity change when curing under different

isothermal conditions; the results are plotted in Fig. 13. The sharp increase of viscosity that is a characteristic of gelling and, therefore, stopping the flow is shifted to shorter times when increasing the curing temperature. Material A is somewhat more reactive than material B, resulting in shorter gelling times. Fig. 14 shows an Arrhenius plot of gel times of both materials.

The activation energies of the curing reactions can be calculated from the slopes of the regression lines plotted in Fig. 14. Similar values of 47 kJ/mol for material A and 46 kJ/mol for material B were obtained.

Based on these measurements, a flow study into large power electronics modules was performed, comparing a variation on component number and topography to yield the optimum filling behavior. The experimental setup for the flow study is shown in Fig. 15, where variants 1-4 are set up to provide information for the mold module layout.

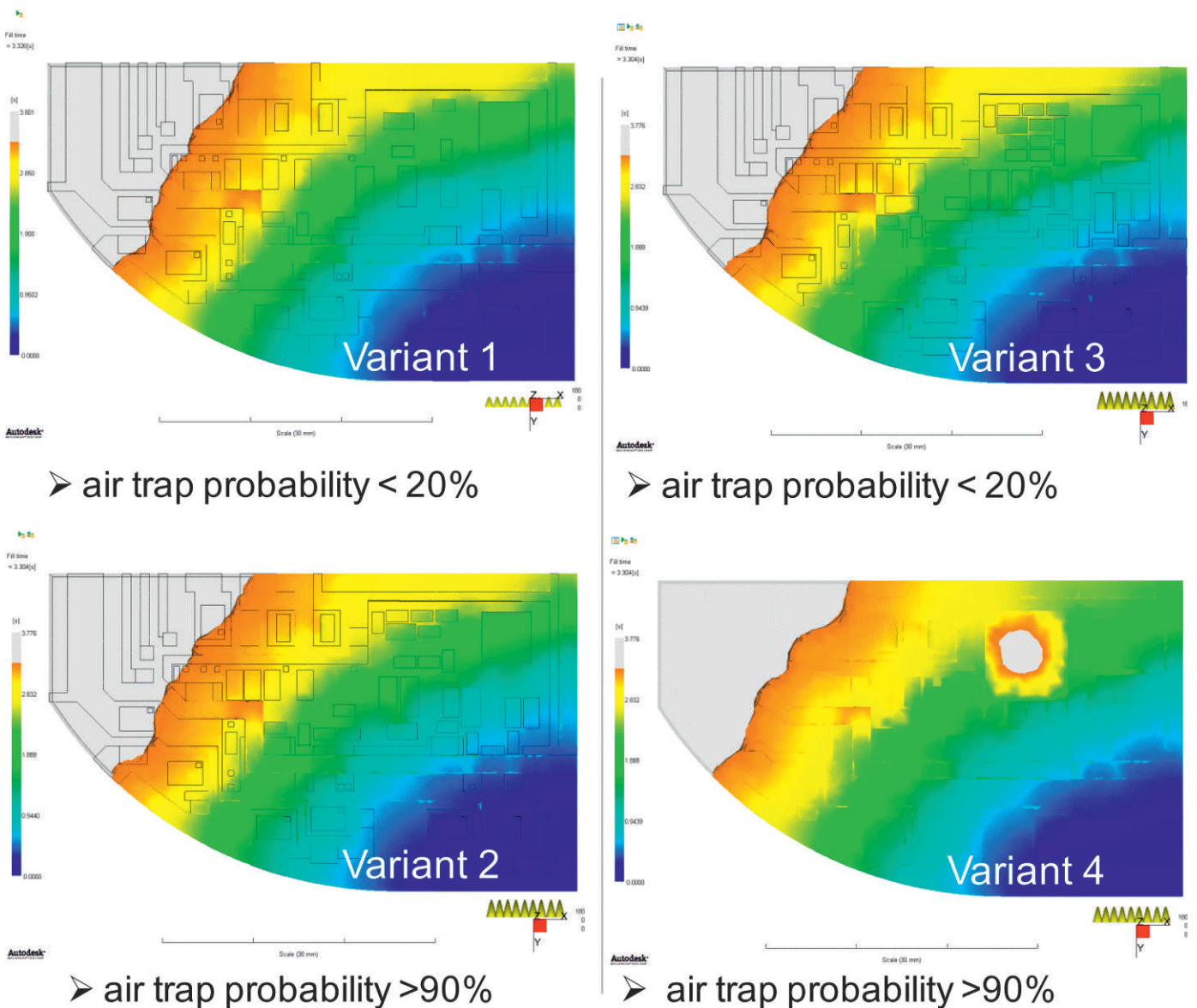


Fig. 16. Flow study results for component type and topography variation.

- A. Variant 1
 1. Low component height, large spacing.
 2. Q: Check flow behavior in channels and tunnels can be observed.
- B. Variant 2
 1. Low component height, tighter spacing.
 2. Q: Check flow behavior in tight spaces (compare with Variant 1).
- C. Variant 3
 1. Higher components, high number of components, blocked flow channels between components.
 2. Q: Check flow behavior at obstacles.
- D. Variant 4
 1. Fewer but higher components, high single component with only 200 μm gap to package surface.
 2. Q: Check voiding performance at high components.

The results of the flow study are depicted in Fig. 16, where it was found that the influence of narrow channels, whether between or above the components, is most likely to lead to air entrapments, as can be seen with the results for variant 2 and variant 4, where the possibility of air entrapments is $\sim 90\%$. The 20% probability found for variants 1 and 3 can be considered uncritical, as there is the option of using vacuum molding to prevent voiding for these cases.

CONCLUSIONS

Within this paper, a smart power module for a maritime logistic application is described as a reference application that is integrating power and control logic inside a lead frame based molded package. Using this package as a demonstrator, a detailed analysis of materials and processes was performed to evaluate not only today's material performance in moderate application scenarios, but also to consider the potential of today's encapsulants for future challenges, for example, for the packaging of SiC power electronics devices.

The test program selected included high temperature storage well above 200°C, media storage in humidity, and storage in brake fluid DOT 4. The results showed that, especially for short term temperature storage (<250 h at 225°C) and humidity storage, there is no major effect on the materials. However, DOT 4 storage at elevated temperatures caused significant changes in material properties—preventing long term use in the harshest environment.

Thermal investigation of the package determined thermal performance of the EMCs to be uncritical in the asymmetric package setup present. The dominant thermal path is not influenced by the molding compound, so no high thermally conductive compound is needed here. Rheological analysis was used to determine flow properties of the EMCs that was a useful input for the flow study performed, taking into account a variation in component size and topography, yielding valuable design rules for the layout of integrated control logic boards.

This work is considered a good basis for future projects where the tools used here will be valuable for the evaluation of future high temperature performance of assemblies containing SiC based power electronics—needing a temperature of use in the range up to 250°C.

REFERENCES

- [1] R. Aschenbrenner, A. Ostmann, K.-F. Becker, C. Kallmayer, E. Jung, M.J. Wolf, "New and emerging technologies for hetero system integration," in *The World of Electronic Packaging and System Integration*, ed. B. Michel, R. Aschenbrenner. Dresden, ddp goldenbogen, pp. 17-26, 2004.
- [2] Strategic Research Agenda 2007. ENIAC (European Nanoelectronics Initiative Advisory Council) Joint Undertaking (Editor), Brussels 2007. <http://www.eniac.eu/web/downloads/SRA2007.pdf>.
- [3] M. Kato, T. Nagahara, H. Kawafuji, T. Nakano, M. Honsberg, New transfer molding PFC series with compact package," Proceedings of PCIM2009, Nuremberg, Germany, 2009.
- [4] K.-H. Lee, S. Fissore, O. Jeon, J. Marcinkowski, "Transfer-molded inverter power module for automotive applications," Proceedings of PCIM 2009, Nuremberg, Germany, 2009.
- [5] S. Post, "PBGA reliability for automotive electronics," Proceedings of the SMTA International 2001, Edina, MN, pp. 339-343, 2001.
- [6] P. McCluskey, K. Mensah, C. O'Connor, F. Lilie, A. Gallo, J. Fink, "Reliability of commercial plastic encapsulated microelectronics at temperatures from 125 °C to 300 °C," Proceedings of the Third European Conference on High Temperature Electronics, HITEN 1999, Berlin, Germany, 1999.
- [7] F. Kremer, A. Schönhals (Eds.), "*Broadband Dielectric Spectroscopy*," Springer, Heidelberg, 2002.
- [8] T. Braun, K.-F. Becker, M. Koch, V. Bader, R. Aschenbrenner, H. Reichl, "Reliability potential of epoxy based encapsulants for automotive applications," Proceedings of ESREF, 2005.
- [9] Y. Huang, D. Bigio, M.G. Pecht. Fill pattern and particle distribution of underfill material," IEEE Transactions on Components and Packaging Technologies, Vol. 27, No. 3, pp. 493-498, 2004.
- [10] S.C. Chen, R.D. Chien, R.I. Tsai, and T.K. Lin, "Preliminary study of polymer melt rheological behavior flowing through micro-channels," International Communications in Heat and Mass Transfer, Vol. 32, pp. 501-510, 2005.